THE UNIVERSITY OF BRITISH COLUMBIA

THE PIEZOMETER CONE PENETRATION TEST

by

Donald G. Gillespie

DEPARTMENT OF CIVIL ENGINEERING
The University of British Columbia
Vancouver , Canada
December , 1981

THE PIEZOMETER CONE PENETRATION TEST

by

DONALD G. GILLESPIE

BASc, The University of British Columbia, 1979

A THESIS SUBMITTED IN PARTIAL FULFILMENT OF

THE REQUIREMENTS FOR THE DEGREE OF

MASTER OF APPLIED SCIENCE

in

THE FACULTY OF GRADUATE STUDIES

DEPARTMENT OF CIVIL ENGINEERING

We accept this thesis as conforming

to the required standard

.....

.....

.....

THE UNIVERSITY OF BRITISH COLUMBIA

December, 1981

Abstract

Deep quasi-static cone penetration tests in saturated soils can develop large excess pore pressures . The level and sign of the excess pore pressures depend on the volume change characteristics,the strength and the permeability of the soil. The recent addition of pore pressure measurements during cone penetration testing adds a new dimension to the interpretation for geotechnical parameters. This report shows how the pore pressure measurements enhance the stratigraphic logging abilities of the cone penetration test.

Calibrations performed on the cone penetrometer are used to show the importance of correcting bearing and friction measurements for pore pressure effects . As well as pore pressure effects the importance of procedure and equipment is discussed.

The use of pore pressure dissipations recorded while penetration is halted is illustrated. Theoretical solutions for pore pressure decay rates are illustrated and results predicting the coefficient of consolidation are compared to laboratory measured values. The coefficient of consolidation predicted from decay rates is shown to compare well with laboratory measured values for the soil in the overconsolidated state.

Contents

List of Tables

List of Figures

Acknowledgements

I would like to express my sincere appreciation and gratitude to Dr.Campanella for suggesting the study and providing both logistical support and guidance throughout.

Much of the work was undertaken with Mr.P.K.Robertson who provided many suggestions and hours of field work. Thanks also go to Mr.Bill Berzins especially for writing the computer graphics routines.

Lastly,special thanks go to my wife Brenda for her support and help with presentation.

Financial support was provided by the Department of Energy Mines and Resources,Canada.

Chapter 1

Introduction

1.1 Historical Development of the Piezometer Cone Test

The static cone penetration test has become the premier logging tool for insitu investigations of soil deposits. Its main advantages over the standard penetration test are the rapidity of the test, its high repeatability, and the continuous nature of the profiles obtained.

Recent research on the static cone penetration test has focussed on the measurement and interpretation of pore water pressures at and around the probe. Knowledge of pore water pressure is fundamental to any effective stress interpretation of the measured parameters. In addition, it has been realized that the measurement of pore water pressure provides an additional parameter to describe the soil behavior.

The proceedings of the European Symposium on Penetration Testing, ESOPT I, included works by Janbu and Senneset 1974 and by Schmertmann 1974. Janbu and Senneset proposed an effective stress interpretation of the static cone penetration test, but concluded that their knowledge of the distribution of pore water pressures around the cone was inadequate. Schmertmann introduced the effects of penetration pore pressure on cone resistance. He discussed some of the parameters that effect the measured pore pressure and showed how the level of pore pressure would change the penetration resistance measured.

At another conference, the ASCE Specialty Conference on Insitu Measurement of Soil Properties, two very significant papers illustrated the use of the piezometer cone. Torstensson 1975 described how continuous information on the soil properties could be obtained from only the dynamic pore pressure record. Wissa et al. 1975 showed how the piezometer cone could be used to obtain equilibrium pore pressures, as well as consolidation characteristics from the pore pressure decay rate.

Until recently, all piezometer cones were either made for the sole purpose of measuring pore pressures or were modified versions of the Fugro electric friction cone, in which the pore pressure measuring system was substituted for the friction sleeve. More recent cones such as the one used in this investigation include both the pore pressure measurement capability, as well as bearing and friction measurements. This paper shows how the addition of the pore pressure measuring system can enhance the cone penetration test.

1.2 Report Organization

A great variety of information can be obtained from different aspects of the cone penetration test; the data can be used in either a quantitative or a qualitative manner, depending on the results required. This report is divided into seven following chapters, each of which outlines some aspect of the test.

Chapter 2 describes the equipment and procedure used during

the investigation. Additional description of specific details of the test is included in other chapters, where appropriate.

Chapter 3 illustrates some examples of dynamic pore pressure records and shows how they can be used in a qualitative manner to enhance the stratigraphic logging capability of the cone penetration test.

Chapter 4 investigates theoretical solutions for the development of pore pressure during steady penetration and compares them to measured values.

Chapter 5 describes the effects of equipment and procedure variation on the results obtained and considers the possibility of hydrofracture during cone penetration.

Chapter 6 compares results obtained from consolidation tests to consolidation characteristics obtained from the rate of excess pore pressure dissipation.

Chapter 7 offers some recommendations on the selection of compressibility characteristics that, when combined with the coefficient of consolidation, can be used to calculate a permeability value.

Chapter 8 includes some additional conclusions and recommendations for further research.

Chapter 2

Equipment and Procedure

2.1 Introduction

The purpose of this paper is not to describe the details of the research and development that have gone into the equipment necessary for the research undertaken, but rather to describe and interpret the results obtained. Some description of the equipment and procedure is, however, necessitated by the tremendous range in equipment and procedure used, all of which are termed piezometer cone logging. This chapter gives a short description of the probe, the driving unit, and the recording devices. It then briefly describes the procedures used in calibration, set up, field testing, and data reduction. A more complete discussion of details, especially concerning the equipment, is provided by Campanella and Robertson 1981. The importance of some of the procedures outlined in this Chapter are further discussed in Chapters 5 and 6.

2.2 The Probe and Recording Units

The piezometer friction probe used is illustrated in Figure 1. The cone has a 60 apex angle, with a 10 cm projected base area. The porous filter element sits immediately behind the cone and is connected hydraulically to the pressure transducer for measuring the pore pressure. The pressure transducer used is a hermetically sealed, all welded, flush diaphragm, absolute pressure type. Friction is measured on a friction sleeve having

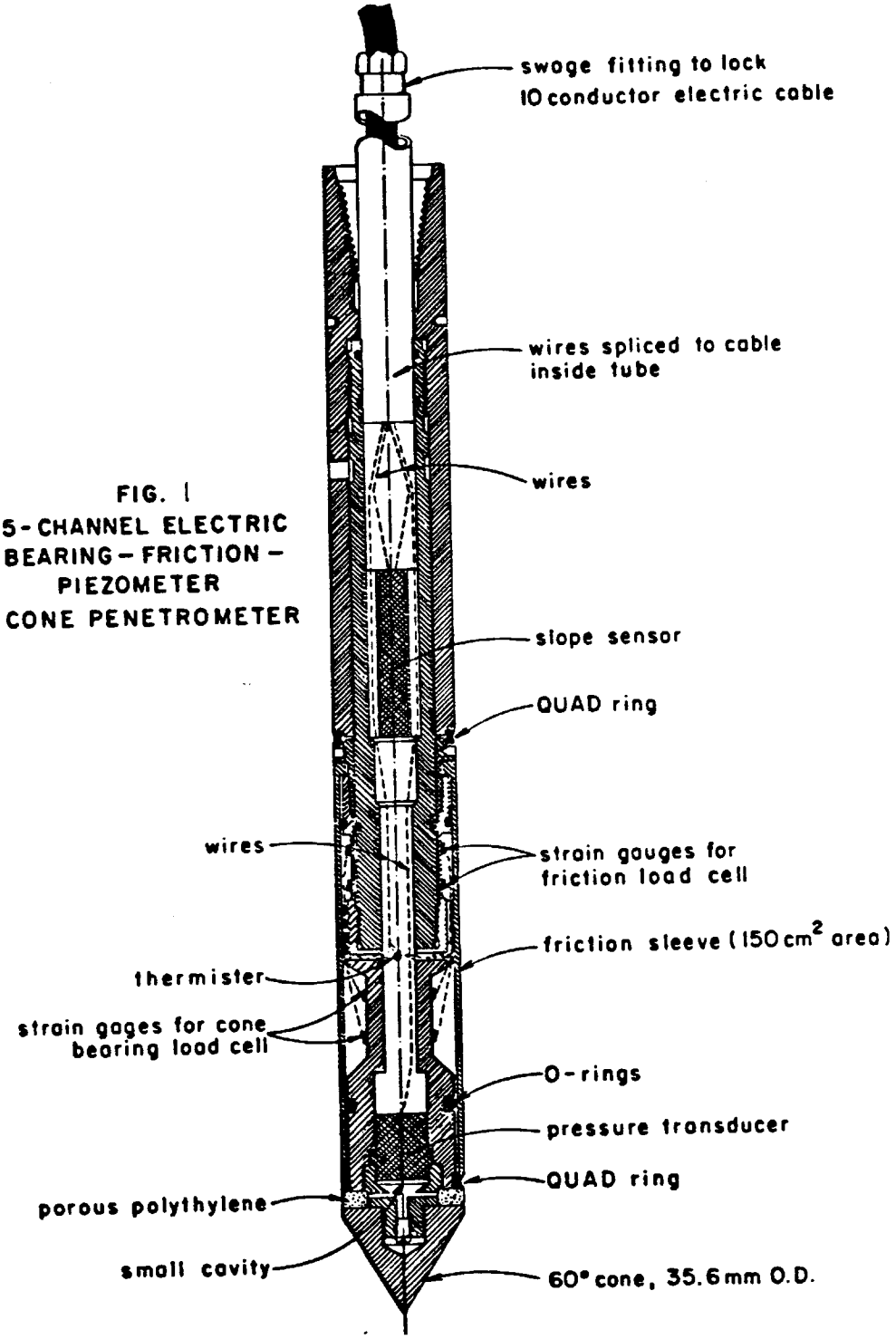

FIG. 1
5-CHANNEL ELECTRIC
BEARING – FRICTION –
PIEZOMETER
CONE PENETROMETER

an area of 150 cm^2.

The capacity of the tip load cell used was 6 tons (about 540 bar), and the capacity of the pressure transducer was 150 psi (10 bar). Although it was not necessary to do so, the pressure transducer was designed to be easily replaced in the field for one of a different capacity.

Signals from the load cells and pressure transducer were sent to the surface through a 10 conductor cable. The use of common excitation permitted the simultaneous measurement of the channels recorded (while only using 8 conductor cables). A 15 volt regulated power supply was used to provide a fixed 10 volt excitation. Balance resistors were used to obtain zero output at the reference setting for each transducer in order to change range on the chart recorder without an offset voltage. Scaling resistors were used to directly plot into engineering units on the chart recorders. Two chart recorders were used in the investigation. One, a three channel recorder driven by a pulse drive-digital shaft encoder, was automatically activated during penetration to record bearing, friction, and dynamic pore pressures with depth. The other recorder was run on a time basis to record pore pressure response during rod breaks and pore pressure dissipation tests. To differentiate between the part of the record that was recorded during penetration from the part that was recorded during rod breaks, each metre of penetration was manually indicated on the record.

To investigate the distribution of pore pressures (and

friction) up the cone shaft, successively longer tip extensions were used to replace the standard cone tip. Addition of the longer cone tips effectively moved both the porous element and the friction sleeve up the cone. The length and arrangement of the cone extensions used is shown in Figure 2. Results of testing conducted with the longer tips is presented in Chapters 5 and 6.

2.3 Driving unit

A complete description of the insitu testing vehicle, its capacity, and hydraulic controls is given by Campanella and Robertson 1981.

2.4 Test Procedure

During the investigation, it was found necessary to pay considerable attention to certain details in the testing procedure. In part, this was necessitated by the extreme range in the parameters measured. For example, the tip load cell had to measure bearing values from 5 to 500 bars. Although not necessary for each field test, the complete procedure required can be broken into four steps: calibration; saturation of the pore pressure measuring system; field testing; and data reduction. Each of these steps is described here because of the sensitivity of the results obtained to their proper completion.

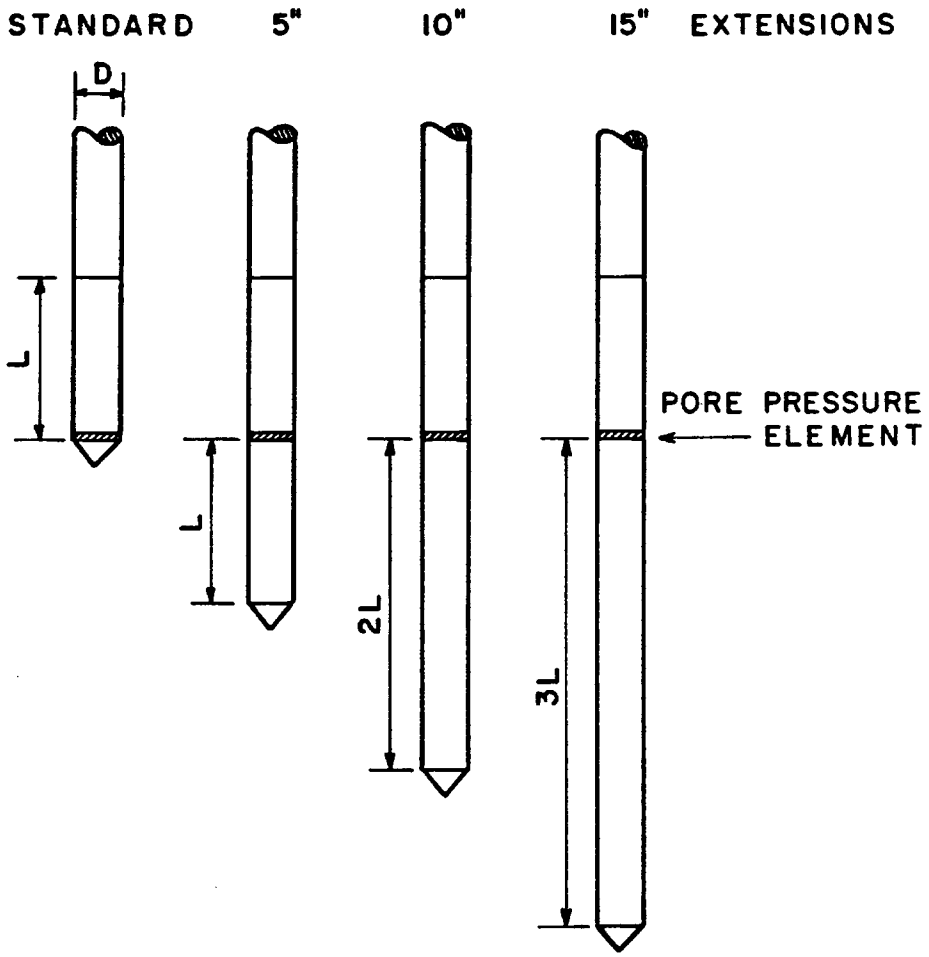

PROBE	FORCES TIP	FORCES SLEEVE
STANDARD	T_A	S_A
5"	$T_A + S_A$	S_B
10"	$T_A + S_A + S_B$	S_C
15"	$T_A + S_A + S_B + S_C$	S_D

FIGURE 2 TIP EXTENSIONS USED

2.4.1 Calibration

Calibration of each of the load cells and the pressure transducer was periodically undertaken to ensure the accuracy of results. To try to reproduce as many field conditions as possible, all calibrations were done in the insitu testing vehicle. During calibration, all voltages were measured on both the chart recorders and a 6 digit multimeter using a 1 microvolt resolution. One of the most important field conditions necessary to duplicate was the use of the 10 channel conductor cable intended for use in the field.

The bearing and friction load cells were calibrated against a reference load cell using a 7 ton calibration jack installed in the testing vehicle. Linearity and stability were found to be excellent. The pressure transducer was calibrated using a dead weight pressure tester connected hydraulically to the pressure transducer. During calibration of each load cell, cross-talk onto the other channels was recorded and found to be insignificant.

During early stages of the investigation, it was found that the tip recorded only about 71% of any water pressure around it. As will be discussed in Chapters 3, 4, and 5, cone penetration testing in cohesive soils generates high pore pressures. Since the tip is a total stress cell, it should record both the soil and water pressure acting upon it. In fact, only 71% of the water pressure was recorded. The explanation of this problem, from which all piezometer cones are thought to suffer, can be

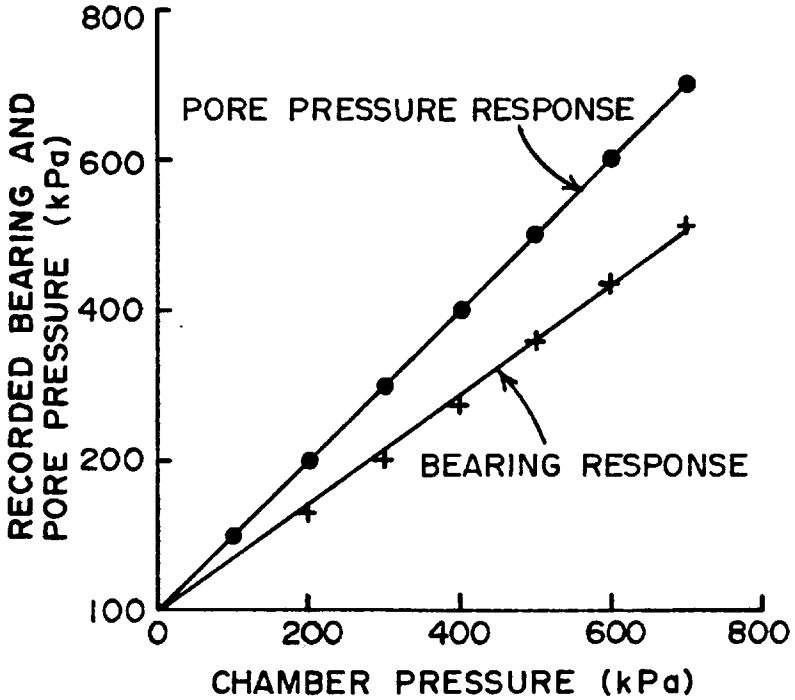

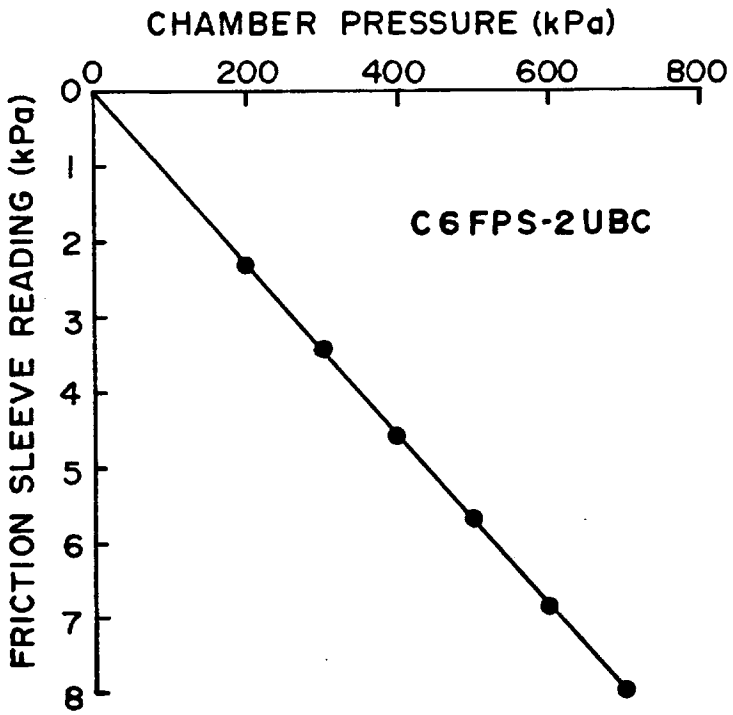

FIGURE 3
RESULTS OF PIEZOMETER FRICTION CONE CALIBRATION.

seen in Figure 3. Some of the pore pressure in the porous element reacts against the friction sleeve and not through the bearing load cell. Figure 3 shows this effect, recorded during calibration of the load cell in a pressure chamber.

Similar hydrostatic pressure corrections were found to be necessary to correct for hydrostatic pressures acting on unequal end areas of the friction sleeve. This calibration, again performed with the cone in a pressure chamber, is shown in Figure 3. Slight nonlinearity in this calibration is due to compressibility of the O and quad rings. These calibration factors are further discussed in Section 2.4.4.

2.4.2 Saturation of the Porous Element

Proper saturation of the pore water pressure measuring system was found to be extremely important for proper interpretation of test results and will be further discussed in Chapter 5.

Glycerine was found to be most effective for saturation. The cavity between the pressure transducer and the porous element was saturated with glycerine using a hypodermic tube when the cone was inverted with the tip and filter removed. When no further air bubbles were seen emerging from the connecting cavities, a saturated porous filter was put into place and the hypodermic entrance was closed with a screw, as shown in Figure 1.

Porous polyethylene and polypropylene filters were used

throughout the investigation. Saturation and cleaning of the elements was achieved by sonically vibrating the porous elements while submerged in glycerine.

2.4.3 Cone Penetration Test Procedure

Following a short warm up period and saturation of the pore pressure measuring system, the cone was attached to the first rod, and the excitation voltages and zeros were adjusted with the cone hanging in a vertical direction. When vertical alignment was ensured, penetration was started. Unless otherwise discussed, the penetration rate used was 2 cm/sec. At one metre intervals, the pushing unit was raised and an additional rod attached. This delay usually took approximately one minute, during which time, pore pressures were recorded. At periodic intervals, penetration was halted, and pore pressure dissipations were recorded with time. During this period, no load was placed on the rods by the pushing head.

At the completion of the test hole, the rods were withdrawn, and, with the cone hanging in the vertical position, the zero load readings were recorded by each channel. Zero drifts were found to be completely the result of temperature variation between the laboratory, where calibration was performed, and the field. The zero used for interpretation of the results obtained was the zero recorded at the test completion, while the cone was still at the ground temperature. Measurement of ground temperatures and possible temperature corrections is given in Campanella and Robertson 1981, who describe a 5 channel cone that includes a thermister.

2.4.4 Data Reduction

The continuous records of bearing friction and pore pressure require considerable handling and reduction, including calculations of the friction ratio, the pore pressure ratio, and the differential pore pressure ratio. To facilitate the calculations required, the strip chart records were digitized on a graphics tablet. During the digitizing process, sufficient data points were used to fully describe the field records; in addition, all unwanted data were eliminated. These unwanted data were caused by loading and unloading at rod breaks. Each of the calculations and corrections performed is described here.

Friction correction

Before calculaing the friction ratio, the friction values were corrected for the pore pressure acting on the exposed differential end areas of the friction sleeve. The equation used was:

$$FC_{Corrected} = FC_{Measured} + 0.011U$$

Consistent units

The pore pressure correction factor, 0.011, was arrived at by applying a hydrostatic pressure to the cone and measuring its effect on the friction sleeve, as described in Section 2.4.1. One assumption inherent in this equation is that the pore pressure, measured just behind the tip, is representative of the pore pressure at the top of the friction sleeve. This important

assumption is further discussed in Chapter 5, in which the distribution of pore pressures up the cone is investigated.

Bearing Correction

The cone penetration tip is a total stress cell; as such, it should record both pore pressure and earth pressure reacting against it. As mentioned in Section 2.4.1, the cone used was found to record approximately 71% of the water pressure acting around it. The proper way, therefore, to account for this is to add to the bearing reading that portion of the water pressure that is not recorded, i.e.:

$$QC_{Corrected} = QC_{Measured} + 0.29U$$

Consistent units

This tip correction is substantial when testing in soft clayey soils, which have high dynamic pore pressures and low bearing values. The importance of this tip correction is further discussed in Chapter 5. It should, however, be noted that the correction factor used, 0.29, was arrived at by calibrating the friction piezometer cone C6FPS-2UBC; other cones, all of which suffer from this problem, may have different correction factors. It is, in fact, the variation in correction factors that necessitates proper bearing and friction corrections.

Differential Pore Pressure

Differential pore pressure is introduced by Campanella et

al. 1981 as being a more fundamental parameter than the dynamic pore pressure. This differential pore pressure is calculated by:

$$U_{Differential} = U_{Measured} - U_{Static}$$

Static pore pressures were interpolated between measured equilibrium values.

Friction Ratio

Friction ratios were calculated using an offset depth of 10 cm between simultaneous (corrected) bearing and friction values. Friction ratios were plotted at the depth of the offset friction reading and calculated using a linearly interpolated value for the bearing.

Pore Pressure Ratio

Pore pressure and differential pore pressure ratios were calculated and plotted at the depth of the pore pressure reading using interpolated values between the nearest digitized bearing values.

Chapter 3

Dynamic Pore Pressures and Stratigraphic Logging

3.1 Introduction

The necessity for monitoring dynamic pore pressures to correct the measured bearing and friction values was shown in Chapter 2. In addition to correcting the bearing and friction values, the dynamic pore pressure log and dissipation records can enhance the stratigraphic logging abilities of the cone penetration test. The use of bearing and friction measurements for stratigraphic logging is thoroughly explained by Schmertmann 1978 and others; this chapter discusses only the ways in which the addition of pore pressure measurements can be useful. The generation of pore pressures is discussed, and the dynamic pore pressure ratio introduced. For illustration purposes, specific examples are drawn upon and explained.

3.2 Pore Pressures Generated During Cone Penetration Testing

Pore pressures generated during cone penetration testing depend upon the material tested and the procedure used. Experience has shown that cone penetration testing in clean sands is essentially a drained test. In contrast, cone penetration testing in clay soils is a fully undrained test. The degree of pore pressure dissipation during testing in intermediate soils is further discussed in Chapter 5. The magnitude and sign (greater or less than the equilibrium pore pressure) is a function of the test procedure, preexisting

stress level, and the material tested. Cone penetration testing in dense sands with sufficient fines content (partially drained) often results in the generation of negative pore pressures, whereas cone penetration testing in loose sands often results in generation of positive pore pressures. As soils become more plastic, positive pore pressures are generated; the magnitude of the pore pressure is discussed in Chapter 4. Pore pressures can also be expressed as a ratio of the bearing value (which should also include the water pressure acting on the tip); this topic is outlined in the next section.

The CPT logs from the Mcdonald site are shown in Figure 4. The site is characterized by silt overlying clean sands to 13 metres. Below 13 metres, the sands grade into silty sands with low bearing values. Below 15 metres, a soft clayey silt deposit can easily be identified by the bearing and pore pressure response, as well as by the friction ratio. Very slightly negative pore pressures ,recored behind the tip,can be seen in the fine silty sand from 13 to 15 metres. Although the sand above has much high bearing values, it is free draining and no negative pore pressures are observed. Even though the two sand deposits, therefore, have similar friction ratios, an indication of their gradational characteristics can be obtained. The soft clayey silt deposits below 15 metres generate large positive pore pressures and can easily be distinguished.

3.3 Dynamic Pore Pressure Ratio

An example showing large pore pressures generated during

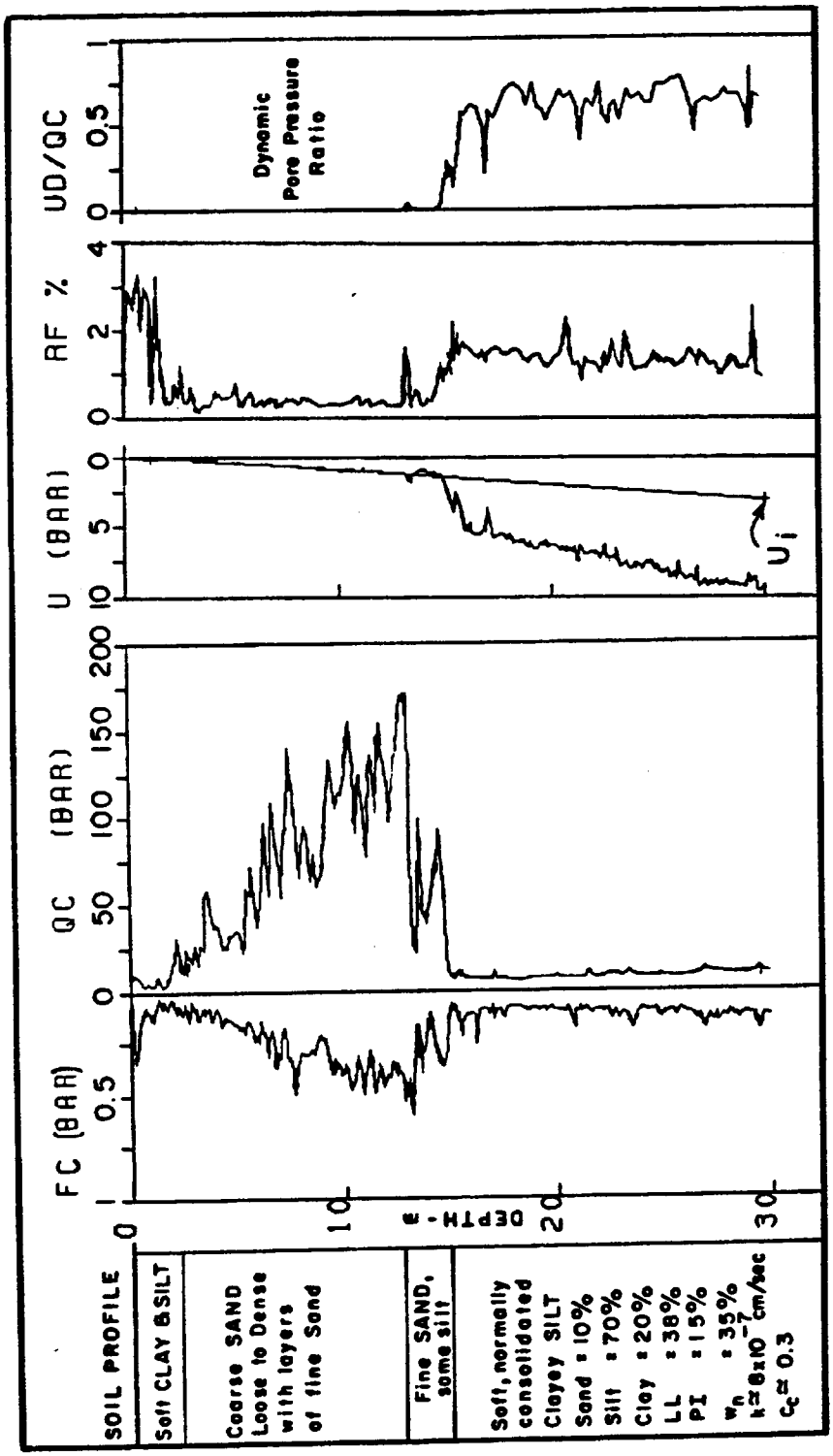

FIG. 4 SOIL PROFILE FOR RESEARCH SITE AT McDONALDS FARM, SEA ISLAND.

cone penetration tests have been shown. For most clayey soils, the undrained shearing results in large pore pressures and accompanying decrease in the effective stress level. The pore pressures generated result from a combination of two factors: The large shear induced pore pressure; and the compressive stress induced pore pressure. Baligh et al. 1980 introduced the pore pressure ratio U/QC as a means of nondimensionalizing the pore pressure generated. It was proposed that, when penetrating soft clayey soils, the shear induced pore pressures would be positive, whereas the shear induced pore pressures generated during cone penetration testing in overconsolidated soils would be small or even negative. This does not imply that the total pore pressure generated need necessarily be negative because of the pore pressures generated by the compressive stresses. As will be shown in Chapter 4, the magnitude of the total pore pressures generated in clayey soils is, to a degree, a function of the undrained shear strength. By expressing the pore pressure as a ratio of the bearing, which is also a function of the undrained shear strength, it was hoped that the effects of shear induced pore pressure and, therefore, stress history could be emphasized. Thus, it was hypothesized that overconsolidated soils that generate small positive or negative pore pressures when sheared and have high bearing values should have a low pore pressure ratio U/QC, whereas soft soils should have a pore pressure ratio approaching 1.0.

Since the bearing value is a combination of soil resistance and water pressure acting on the tip, the upper limit of the

pore pressure ratio is 1.0. In spite of this, pore pressure ratios greater than 1.0 are commonly reported. A list of pore pressure ratios is shown with measured overconsolidation ratios:

		OCR	U/QC
Baligh *et al.*	1980	6	0.6
60° Tip		4	1.0
		2	1.2
Baligh *et al.*	1980	6	0.15
18° Tip		4	0.4
		2	0.75
Lacasse *et al.*	1981	2.5	0.5
		1.5 - 1.15	0.6
		1.2	0.7
Roy *et al.*	1980	2.2 - 2.5	0.56
This Investigation		1.0	0.8 - 1.0

The differential pore pressure ratio--the ratio of that pore pressure in excess of the hydrostatic value to the bearing value--was introduced by Campanella *et al.* 1981 as being a more fundamental parameter.

Cone penetration testing in granular materials may also generate either positive or negative pore pressures. In sands,

the bearing value is usually so large and the induced pore pressure so low that the ratio (either positive or negative) is usually very small. Mixed soils may, however, result in larger pore pressure ratios, which could have a value similar to that of an overconsolidated clay. Differentiation between an overconsolidated clay soil and a silty soil may not be possible if only the dynamic pore pressure and bearing values are available. Differentiation between such soils is, however, possible with the aid of friction measurements and the friction ratio. Possible additional means of differentiating such soils using pore pressure decay rates is described in Chapter 6.

3.4 Stratigraphic Logging

Specific examples of the usefulness of simultaneous measurements of dynamic pore pressures,recorded behind the tip, as well as friction and bearing values, are presented in this section.

3.4.1 CPT Example 1 Figure 5

The complete cone log obtained from a site of the Fraser River delta is shown in Figure 5. The interbedded sands and silts were deposited since the last glacial period. The stratigraphic variation shown results, in part, from variation in the location of the river channel within the prograding delta. The material types interpreted from the cone logs are shown in Figure 5. Within each unit shown, the greatest detail can be seen from the pore pressure log. For example, within the

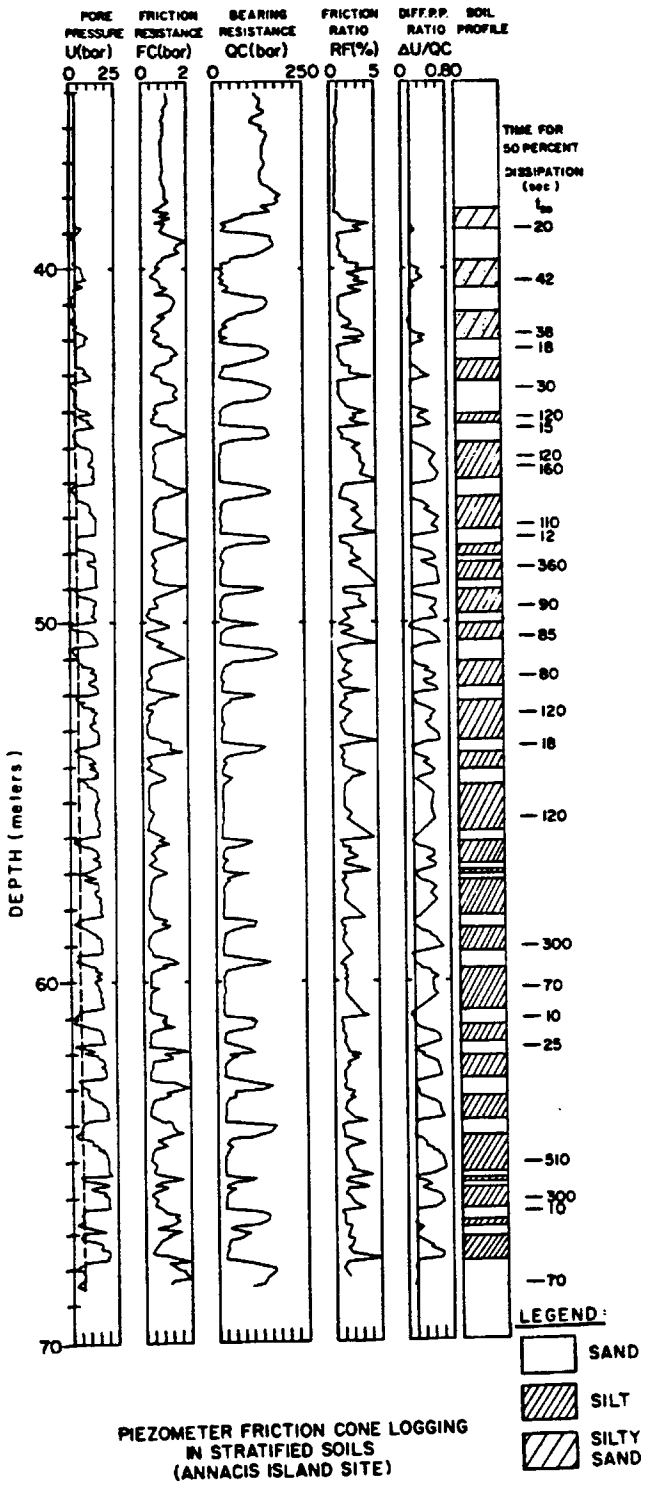

PIEZOMETER FRICTION CONE LOGGING
IN STRATIFIED SOILS
(ANNACIS ISLAND SITE)

FIGURE 5 CPT EXAMPLE I

silt lenses, the bearing and friction values, which reflect the properties of a larger zone of soil, are nearly constant, whereas the pore pressure log reveals small sandier partings within each silt lens.

The material classification shown in Figure 5 includes the distinction between sand, silt, and silty sand deposits. Although the sand and silt deposits are easily distinguished using only the bearing and friction measurements, the silty sand layers can only be distinguished from the silt layers by the pore pressure measurements. The bearing and friction ratio for the two materials are similar; each has a value of approximately 20 bar and 3.0 respectively. If only the friction and bearing measurements are available, each would be classified as a silt. Inspection of the dynamic pore pressure logs, however, reveals a distinctly different behavior of the two materials. Compared to the silt, the silty sand has a much lower dynamic pore pressure. The variation in dynamic pore pressure can occur because either the silty sand is less compressible or is a more freely draining material. Since the materials have equivalent bearing values, it appears that penetration of the silty sand results in a lower dynamic pore pressure because of partial drainage of the dynamic pore pressures. A more complete indication of the gradational characteristics can thus be obtained from the pore pressure response.

An alternate means of identifying the three soil types can be obtained from the time to reach dissipation of 50% of the excess pore pressure, t_{50}, such as those marked at their

appropriate depths in Figure 5. For a given probe, the time for dissipation of 50% of the excess pore pressure is a function of the consolidation characteristics of the soil, and clearly distinguishes the three soil types. The location of the pore pressure dissipations shown in Figure 5 also highlights the necessity of inspecting the complete cone logs when interpreting dissipation test results. Dissipations conducted within the silt lenses, but near sand boundaries, are affected by the greatly reduced drainage path length.

The time to reach t_{50} is a useful parameter for distinguishing stratigraphic types. For many soil types such as those shown in Figure 5, the time to reach 50% dissipation of excess pore pressure is often achieved during rod breaks, with very little standby time. Similar results can be obtained using a smaller degree of dissipation in less permeable soils.

3.4.2 CPT Example 2 Figure 6

A generalized soil profile for this site would indicate that the site could be broken into two basic units: a sand deposit overlying silt, with interbedded sand lenses. The sand lenses are easily distinguished by their high bearing, low friction ratio, and low differential pore pressure ratio. The silt has bearing values ranging from 20 to 30 bar, increasing with depth, and is easily distinguished by its high dynamic pore pressure ratio. In contrast to the silt deposits, a very low bearing value material can be seen between 28.5 and 30.0 metres. The bearing and friction ratios alone indicate that the material

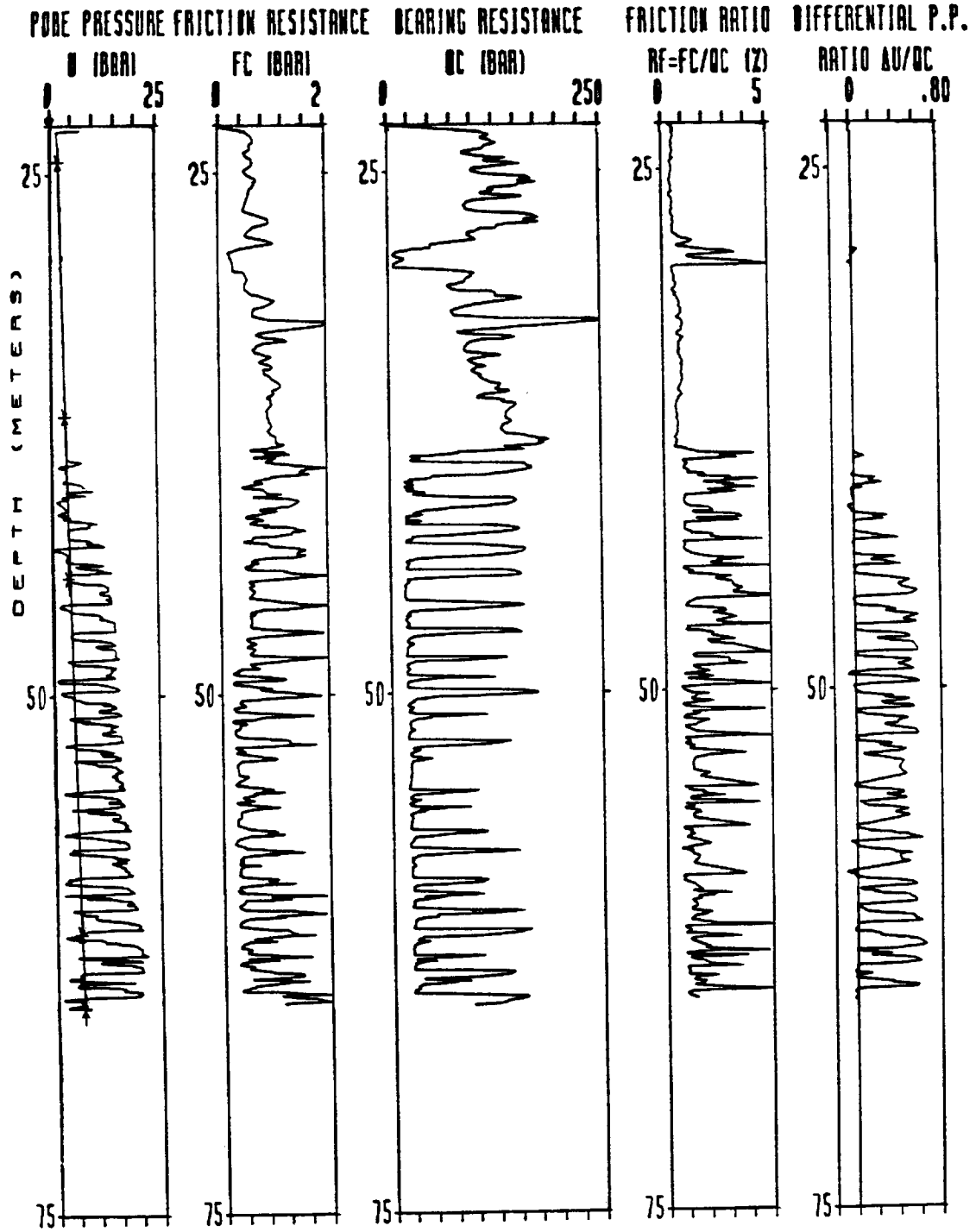

FIGURE 6 CPT EXAMPLE 2

is a soft clay soil; examination of the pore pressure record, however, shows that no pore pressure was generated during penetration. Two very distinct types of material do not generate excess pore pressures when sheared: those that are so free draining that the pore pressures immediately dissipate; and those that are of a particular stiffness such that neither positive nor negative pore pressures result. Since material with a much higher bearing value--the silt lenses between 45 and 70 metres--results in very large pore pressures, it appears that the material between 28.5 and 30.0 metres is a free draining, but very soft, material. The bearing value is too low and the friction ratio too high for the material to be a sand. It would appear, therefore, that the material is a free draining organic deposit such as fibrous peat.

3.4.3 CPT Example 3 Figure 7

Pore pressure records, especially dissipations, are sensitive to both the material that the piezometer element lies within and the material surrounding the cone. To illustrate some of the effects of soil stratigraphy on the pore pressure response, Figure 7 shows a portion of the dynamic pore pressure record. As indicated in Figure 7, the record includes both the dynamic pore pressure record with depth, as well as the dissipation records obtained during rod breaks. Dissipations conducted at 73.6 and 75.6 metres are of the type generally recorded in a clayey deposit. Dissipations of the type recorded at 74.6 metres, however, have also been shown in the literature.

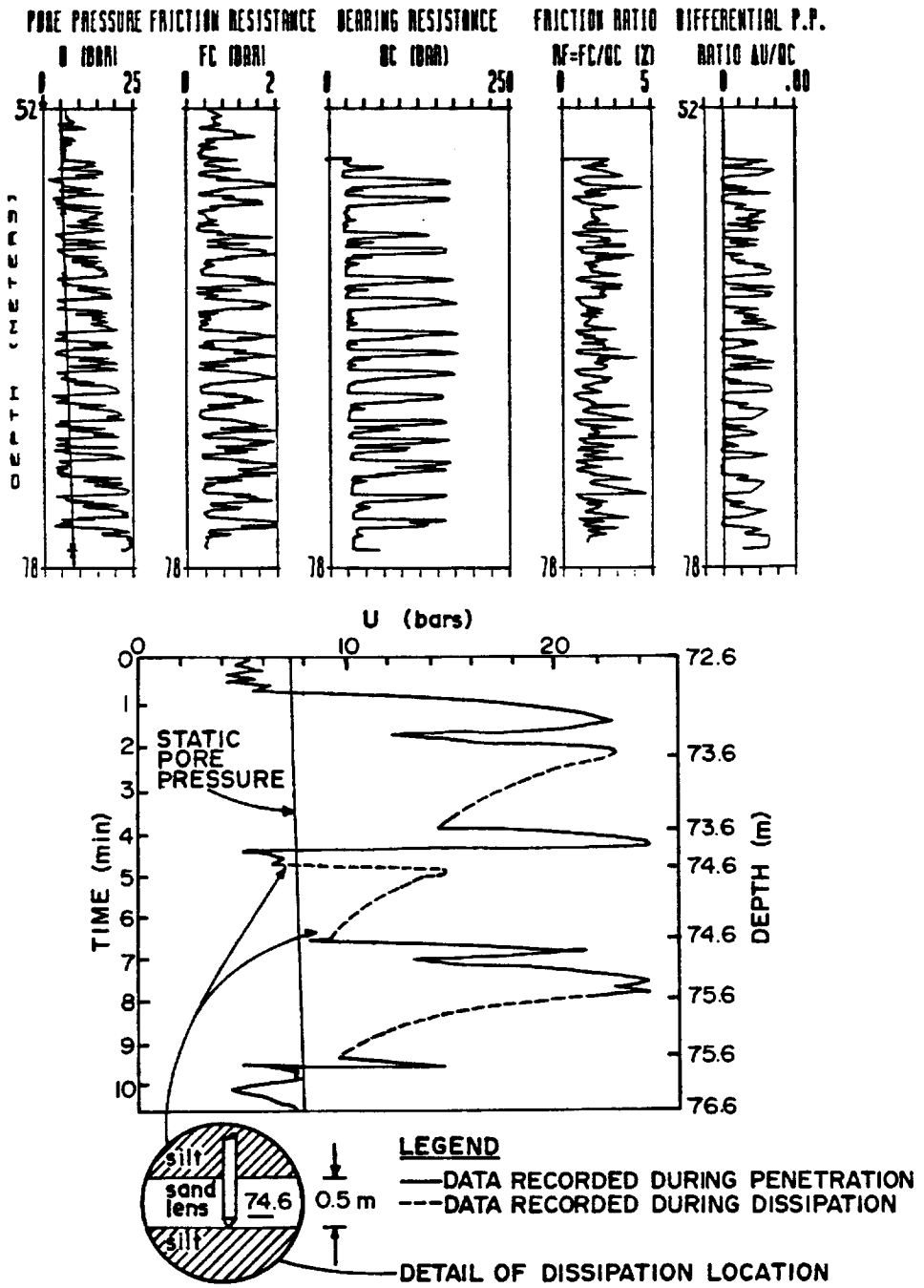

FIGURE 7: COMPLETE CPT LOG AND DETAIL OF DYNAMIC PORE PRESSURE RECORD

Many explanations exist for the apparent increase in pore pressure before the ultimate decay of excess pore pressure. In this case, however, examination of the complete depth recordings reveals that the piezometer element at 74.6 metres was within a sand lens. As shown in Figure 7, pore pressures generated in the silt lens, both above and immediately below the cone, resulted in a delayed pore pressure rise in the sand lens after penetration was halted. Subsequent rapid dissipation of pore pressure was controlled, in part, by the higher permeability of the sand lens. Other dissipations of this type are often seen in layered soils; careful examination of the complete records, both with depth and with time, can further explain such phenomena.

3.4.4 CPT Example 4 Figure 8

Figure 8 shows the bearing and pore pressure logs obtained before and after compaction in adjacent holes. The material was hydraulically placed. It has been stated that when shearing soils of sufficiently low permeability, dynamic pore pressures result, the level of which depends on the volume change characteristics of the soil. Figure 8 illustrates the change in both magnitude and sign of the dynamic pore pressure that accompanies an increase in compactiveness of the soil. Before compaction, large positive pore pressures are generated in the soft silt between 2.5 and 7.5 metres; after compaction, the dynamic pore pressures become negative. Although the magnitude and sign of the dynamic pore pressure has only been used to date

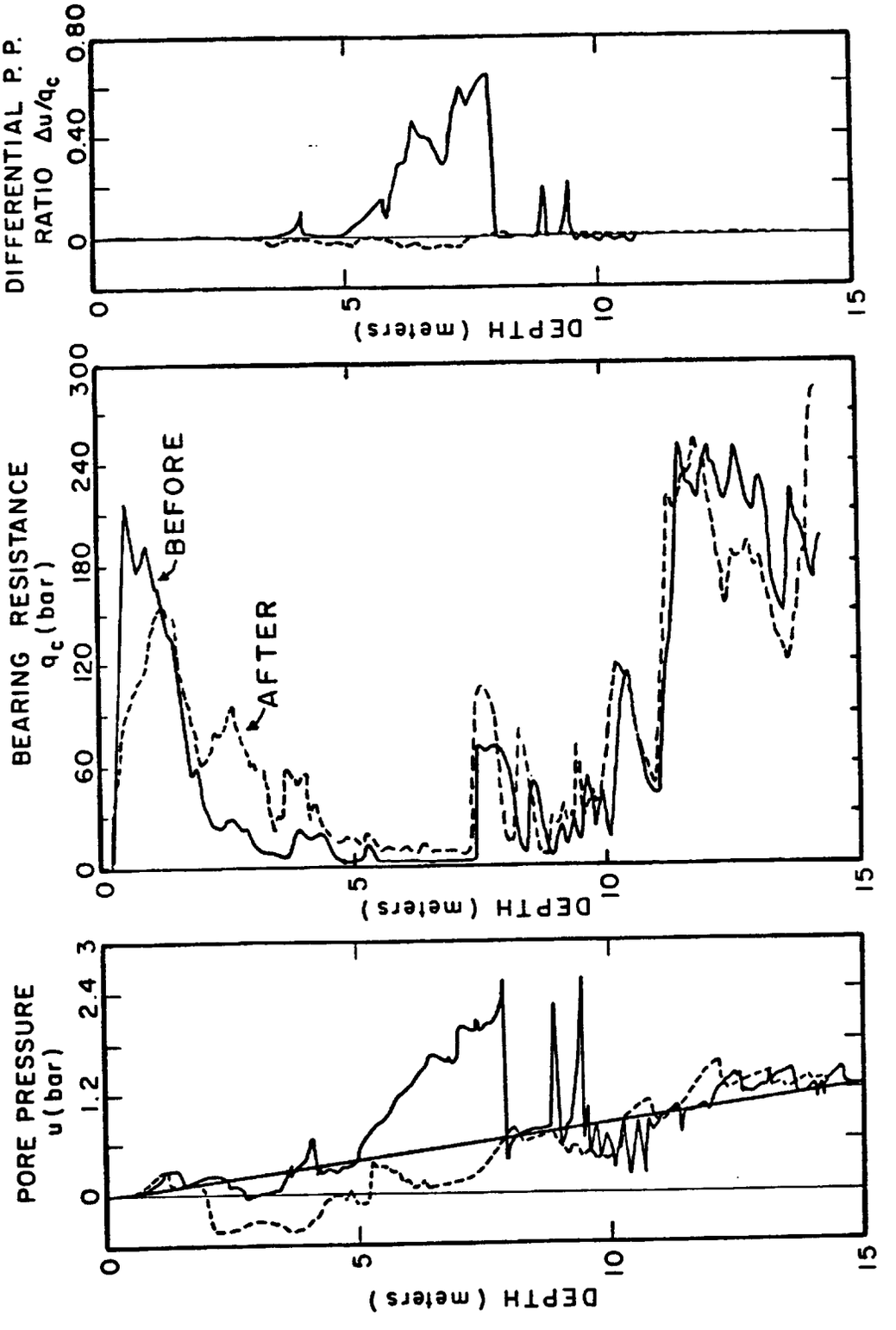

FIGURE 8 BEFORE & AFTER COMPACTION CPT EXAMPLE 4

in a qualitative manner, it may prove to be a useful parameter to describe the properties of partially drained or undrained materials.

The sign of the dynamic pore pressure probably depends on the location of the measuring element. As stated in Campanella et al. 1981, the location of the porous element used in this investigation probably encourages the measurement of negative pore pressures in all but very loose soils. Further investigation of the effect of location of the porous element is ongoing.

3.5 Static Pore Pressures

Piezometer cone logging can be stopped at any depth and the equilibrium ground water conditions measured. Although the cone generates dynamic pore pressures during penetration, careful monitoring of the decay of excess pore pressure with time can ensure that full equilibrium has been achieved. In this manner, cone penetration testing can be a cost effective means of obtaining equilibrium ground water conditions. As will be shown in Chapter 6, the time to achieve any degree of dissipation is a function of the consolidation characteristics of the soil and the radius of the probe squared. The fact that the time to reach equilibrium conditions increase with the radius of the probe squared is one of the reasons why early piezometer probes, which only measured pore pressures, were of very small radius.

An example of the use of the piezometer cone for obtaining

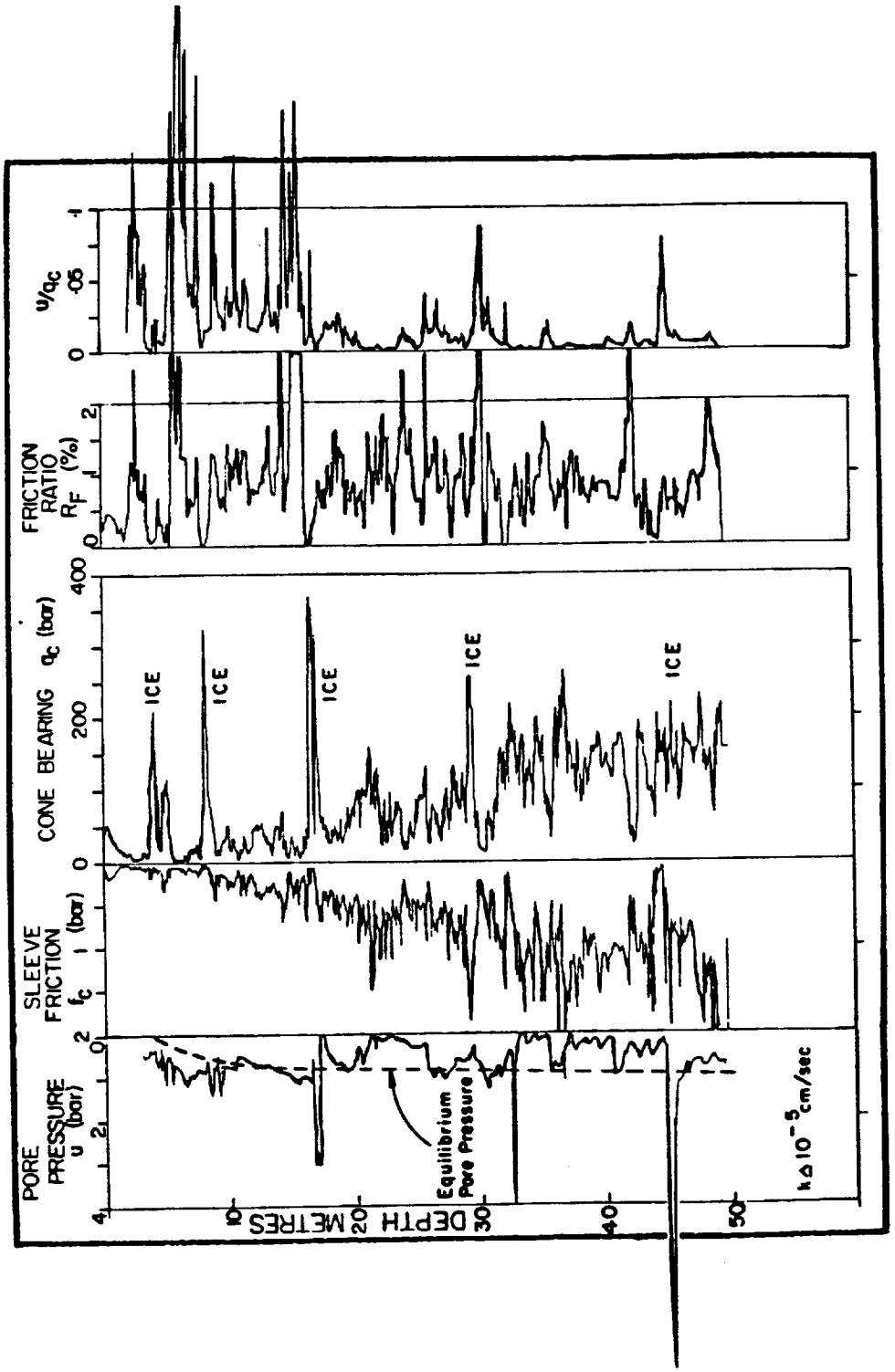

FIG. 9 EXAMPLE OF PIEZOMETER, FRICTION CONE LOG THROUGH TAILINGS DEPOSIT.

Chapter 4

Analytical Expressions for Dynamic Pore Pressure

4.1 Introduction

During cone penetration testing, pore pressures have only been measured at one location. The location chosen during this investigation was directly behind the tip. In addition, pore pressures were also measured up the shaft. Other researchers, Roy et al. 1980 and Baligh et al. 1980, have measured pore pressures at the tip of the cone penetrometer. Alignment problems preclude the possibility of actually measuring pore pressures around the cone during cone penetration testing. Previous experience in measurement of pore pressures around driven piles can, however, be drawn upon to compare pore pressures with radial distance from the cone to those measured at the cone surface. This chapter compares analytical expressions for the magnitude and distribution of pore pressures with field observations of dynamic pore pressures around driven piles. In addition, analytical expressions for the magnitude of the pore pressure generated are compared with values measured during cone penetration testing at the Mcdonald site.

A knowledge of the magnitude and distribution of pore pressures is important for several reasons, including:

1) The distribution of dynamic pore pressures represents the initial conditions for pore pressure dissipation analysis used to calculate consolidation

characteristics.

2) Penetration testing influences a large zone of soil; the distribution of pore pressures is fundamental to any effective stress interpretation of bearing and friction measurements.
3) If analytical expressions for the generated pore pressure that rely on fundamental soil properties compare well with measured pore pressures generated at the surface of the cone, then dynamic pore pressure measurement may prove useful in evaluating soil parameters.

4.2 Analytical Expressions

The theoretical prediction of the pore pressure distribution induced during steady cone penetration testing in saturated clayey soils is the subject of considerable attention because of its relevance to many problems, including pile installation and the interpretation of insitu tests, which include the piezometer cone and the pressuremeter tests. Pore pressure distribution around the cone penetrometer is complicated by:

1) complex boundary conditions around the cone;
2) complex stress paths followed by the soil, especially near the cone;
3) very large strains; and
4) complexity of soil behavior.

In order to simplify the problem, several assumptions must be made regarding both the soil behavior and geometry.

Experience gained by monitoring of pore pressures induced by driven piles has led to the relatively widely accepted idea that the complex geometry of cone installation can be modelled by either expansion of a cylindrical or spherical cavity. Past experience seems to indicate that pore pressures generated at the tip can best be estimated by expansions of a spherical cavity, whereas pore pressures up the sleeve or shaft can best be modelled by expansion of a cylindrical cavity (Roy et al. 1980 and Vesic 1972).

In addition to simplification of the geometry, different soil models can be used to describe the soil behavior. This section summarizes analytical expressions for pore pressure magnitude and distribution. Chapter3 showed examples of very low dynamic pore pressure recored when penetrating certian clayey soils. Negative dynamic pore pressures were observed when penetrating a compacted silty soil. Other researchers have shown how the dynamic pore pressure,especially when expressed as the dynamic pore pressure ratio,decreases with increasing overconsolidation ratio for a clay soil. Some of the analytical expressions illustrated in this Chapter apply only to normally consolidated soils. Others attempt to account for the volume change characteristics of the soil,the difference between the expressions should be noted.

4.2.1 Comparison between Models

A rigorous comparison between models is dependent upon the selection of input parameters. Recognizing that no single test procedure can result in a reference parameter, Table I summarizes the selection of input parameters and the predicted level of excess pore pressure for each of the models outlined. The results are shown for the silt at 20 metres depth. Comparison between models and measured pore pressures at the Mcdonald site is discussed further.

Parameters Used

cu undrained shear strength

Ir rigidity index = E/3cu

E elastic modulus - undrained

U pore pressure

r radial stress

p average stress

A_f Skempton's pore pressure parameter

k at rest earth pressure ratio

Geometric Terms

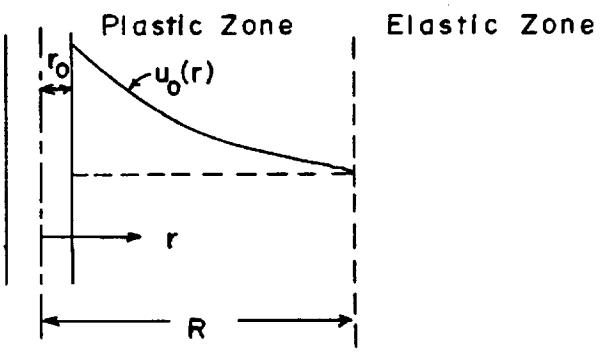

MODEL	Parameters Used (bar) cu	Ir	Af	ϕ'	$\frac{p'_{cs}}{p'_{nc}}$	U cyl	Usph
1. Elastic plastic	0.55	167				2.81	3.75
2. Elastic plastic with volume hardening	0.55	167			0.4	3.26	4.20
3. Semi empirical Torstensson 1977	0.55	167	1.0			3.45	4.49
4. Semi empirical Hagerty and Garlanger 1972	0.55			32°		1.94	
5. Semi empirical Roy et al. 1979			U/p =0.75			2.33	

Material Tested — Clayey Silt — QC = 8.2 bar
σ_v' = 2.0 bar — PI = 15% — % sand 10
U_o = 2.0 bar — LL = 38% — % silt 70
Wn = 35% — % clay 20

-cu = QC/NC = 8.2/15 =0.55 bar lab vane 5--6 bar
-Ir = Estimated from Correlations between cu and Ir from Ladd et al. 1977
-Af = Estimated from correlations between OCR and Af, Lambe and Whitman 1969
-ϕ' = Estimated from correlations between PI and ϕ', Lambe and Whitman 1969
-$\frac{p'_{cs}}{p'_{nc}}$ = Estimated from correlations between p'_{cs}/p'_{nc} and Cc, Esrig and Kirby 1978

Table I Input Parameters Used to Compare Dynamic Pore Pressure Models

Method 1 Elastic perfectly plastic soil

Vesic 1972; Randolph and Wroth 1979;

Torstensson 1977

Cylindrical cavity

$$\Delta \sigma r = cu(1 + \ln Ir) \quad (1)$$

$$\Delta U = 2cu \cdot \ln R/r \quad (2)$$

$$R/r = (Ir)^{1/2} \quad (3)$$

Spherical cavity

$$\Delta \sigma r = 4/3cu(1 + \ln Ir) \quad (4)$$

$$\Delta U = 4cu \ln(R/r) \quad (5)$$

$$R/r = Ir^{1/3} \quad (6)$$

Method 2 Elastic plastic soil with volume

hardening soils with OCR < 2.0

Schofield and Wroth 1968; Roscoe and Burland 1968

$$\Delta U = (p'_i - p'_f) + \Delta p \quad (7)$$

$$M = q/p = 6 \sin \phi'/(3 - \sin\phi) \quad (8)$$

$$q = \sqrt{3}cu \quad (9)$$

$$\Delta p = \text{from eqns } \underline{2} + \underline{4} \quad (10)$$

Cylindrical cavity: after Esrig and Kirby 1978

$$\Delta U = (p'_i - p'_f) + \Delta p \quad (11)$$

$$\Delta U = (p'_{nc} - p'_{cs}) + 2cu \ln Ir^{1/2} \quad (12)$$

$$\Delta U = \frac{\frac{p'_{nc}}{p'_{nc}} - \frac{p'_{cs}}{p'_{nc}}}{p'_{nc}} + 2cu \ln Ir^{1/3} \quad (13)$$

Spherical cavity: after Esrig and Kirby 1978

$$\Delta U = (p'_i - p'_f) + \Delta p \qquad (14)$$

$$\Delta U = (p'_{nc} - p'_{cs}) + 4cu \ln Ir^{1/3} \qquad (15)$$

$$\Delta U = \frac{\frac{p'_{nc}}{p'_{nc}} - \frac{p'_{cs}}{p'_{nc}}}{p'_{nc}} + 4cu \ln Ir^{1/3} \qquad (16)$$

Method 3 Semi empirical

Torstensson 1977;Massarch 1978

$$\Delta U = 1/3(\Delta \sigma_1 + \Delta \sigma_2 + \Delta \sigma_3) + a_f [(\Delta \sigma_1 - \Delta \sigma_3)^2 + (\Delta \sigma_2 - \Delta \sigma_3)^2 + (\Delta \sigma_1 - \Delta \sigma_2)^2]^{1/2} \qquad (17)$$

$$a_f = 1/2(3A_f - 1) \qquad (18)$$

Cylindrical cavity

$$\Delta U = cu[\ln Ir + 0.577(3A_f - 1)] \qquad (19)$$

Spherical cavity

$$\Delta U = cu[4/3 \ln Ir + 0.667(3A_f - 1)] \qquad (20)$$

Method 4 Semi empirical

Hagerty and Garlanger 1972

Cylindrical cavity

$$\Delta U = p'_o [1 - (\sin \phi' / \sin \phi') \cdot Cu/p'_o)] \qquad (21)$$

Method 5 Semi empirical

Roy et al. 1979

Cylindrical cavity

$$\Delta U = (1 - k)\sigma_{v'o} + (\Delta U/p)m\sigma'p \qquad (22)$$

Calculated values for the differential pore pressure, ($U_{Measured} - U_{Static}$) are shown for the clayey silt at the Mcdonald site in Table I. As can be seen in the analytical expressions for the dynamic pore pressure, the models are not sensitive to the selection of a rigidity index (stiffness ratio); they are, however sensitive to the selection of an undrained shear strength. The undrained shear strength used was calculated from the measured bearing value. The effect of increased rigidity index is mainly to extend the zone of soil influenced by the cavity expansion. Further discussion of the importance of the rigidity index will be included in Chapter 6.

Analytical estimates of the dynamic pore pressure can be compared to the field measured values shown in Figure 10. For the purposes of illustration, only the solutions obtained using the elastic plastic model are shown in Figure 10. The spherical cavity expansion solution compares favourably with the pore pressures measured immediately behind the cone tip. The solution for the cylindrical expansion compares well with pore pressures measured 25 cm (7.1d) behind the cone tip.

An absolute comparison between the results obtained with each model is complicated by the selection of input parameters, especially the undrained shear strength. The elastic perfectly plastic model predicts values very close to the field measured

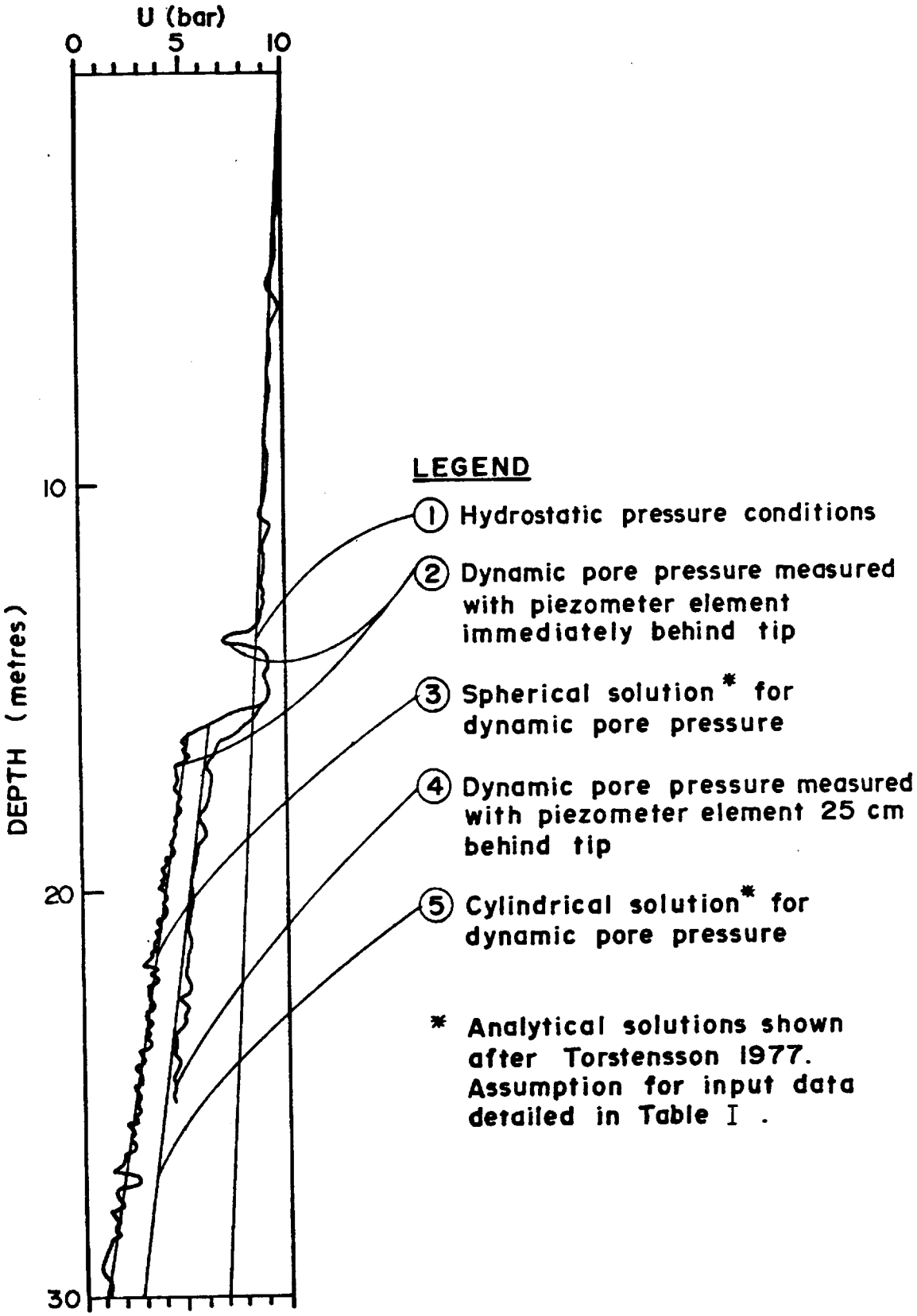

FIGURE 10
COMPARISON BETWEEN ANALYTICAL SOLUTIONS AND MEASURED DYNAMIC PORE PRESSURES.

values. The elastic plastic model with volume hardening predicts slightly high limit and pore pressures. The semi empirical method outlined by Massarch 1978, and Torstensson 1977 includes Skempton's A_f pore pressure parameter. The incorporation of an A_f value, which varies with past loading history, into the expression for dynamic pore pressures is consistent with the belief that the dynamic pore pressure ratio U/QC is a good indicator of the loading history of the soil.

The semi empirical method proposed by Roy et al. 1979 requires an estimate for U/p, best obtained from an undrained triaxial test. As in the case of models by Vesic 1972, Massarch 1978, and Torstensson 1977, which incorporate an A_f value, the model by Roy et al. 1979 attempts to incorporate the effect of previous loading history.

The semi empirical method proposed by Hagerty and Garlanger 1972 tends to underpredict the dynamic pore pressures.

Use of either of the first three models outlined appears to confirm that the pore pressures at the tip can best be modelled by spherical cavity expansion, whereas those measured some distance behind the tip can best be modelled by cylindrical cavity expansion.

The distribution of pore pressures predicted by the models can be compared to pore pressures measured during the installation of piles. Figure 11 shows the distribution of pore pressure around driven piles. Each of the case histories selected confirms the distribution of pore pressure predicted by

the analytical expression (egns 2, 5). The excess pore pressures shown in Figure 11 all appear to decrease with the logarithm of the radius. As previously stated, a knowledge of the initial distribution of excess pore pressures is fundamental to the proper interpretation of pore pressure decay rates.